



# *Plasmodium yoelii* Erythrocyte-Binding-like Protein Modulates Host Cell Membrane Structure, Immunity, and Disease Severity

Yu-chih Peng,<sup>a</sup> Yanwei Qi,<sup>a,b</sup> Cui Zhang,<sup>a</sup> Xiangyu Yao,<sup>a</sup> Jian Wu,<sup>a</sup> Sittiporn Pattaradilokrat,<sup>a,c</sup> Lu Xia,<sup>a,d</sup> Keyla C. Tumas,<sup>a</sup> Xiao He,<sup>a</sup> Takahiro Ishizaki,<sup>e,f</sup> Chen-Feng Qi,<sup>g</sup>  Anthony A. Holder,<sup>h</sup>  Timothy G. Myers,<sup>i</sup> Carole A. Long,<sup>a</sup> Osamu Kaneko,<sup>e,f</sup> Jian Li,<sup>j</sup> Xin-zhuan Su<sup>a</sup>

<sup>a</sup>Malaria Functional Genomics Section, Laboratory of Malaria and Vector Research, National Institute of Allergy and Infectious Diseases, National Institutes of Health, Bethesda, Maryland, USA

<sup>b</sup>Department of Pathogenic Biology and Immunology, Guangdong Provincial Key Laboratory of Allergy and Clinical Immunology, Sino-French Hoffmann Institute, Second Affiliated Hospital, Guangzhou Medical University, Guangzhou, China

<sup>c</sup>Department of Biology, Faculty of Science, Chulalongkorn University, Bangkok, Thailand

<sup>d</sup>State Key Laboratory of Medical Genetics, Xiangya School of Medicine, Central South University, Changsha, Hunan, China

<sup>e</sup>Department of Protozoology, Institute of Tropical Medicine (NEKKEN), Nagasaki University, Nagasaki, Japan

<sup>f</sup>Leading Program, Graduate School of Biomedical Sciences, Nagasaki University, Nagasaki, Japan

<sup>g</sup>Laboratory of Immunogenetics, National Institute of Allergy and Infectious Diseases, National Institutes of Health, Bethesda, Maryland, USA

<sup>h</sup>Malaria Parasitology Laboratory, The Francis Crick Institute, London, United Kingdom

<sup>i</sup>Genomic Technologies Section, Research Technologies Branch, National Institute of Allergy and Infectious Diseases, National Institutes of Health, Bethesda, Maryland, USA

<sup>j</sup>State Key Laboratory of Cellular Stress Biology, Innovation Center for Cell Signaling Network, School of Life Sciences, Xiamen University, Xiamen, Fujian, China

Yu-chih Peng and Yanwei Qi contributed approximately equally to this work. Author order was determined by the time spent on the project and in order of increasing seniority.

**ABSTRACT** Erythrocyte-binding-like (EBL) proteins are known to play an important role in malaria parasite invasion of red blood cells (RBCs); however, any roles of EBL proteins in regulating host immune responses remain unknown. Here, we show that *Plasmodium yoelii* EBL (PyEBL) can shape disease severity by modulating the surface structure of infected RBCs (iRBCs) and host immune responses. We identified an amino acid substitution (a change of C to Y at position 741 [C741Y]) in the protein trafficking domain of PyEBL between isogenic *P. yoelii nigeriensis* strain N67 and N67C parasites that produce different disease phenotypes in C57BL/6 mice. Exchanges of the C741Y alleles altered parasite growth and host survival accordingly. The C741Y substitution also changed protein processing and trafficking in merozoites and in the cytoplasm of iRBCs, reduced PyEBL binding to band 3, increased phosphatidylserine (PS) surface exposure, and elevated the osmotic fragility of iRBCs, but it did not affect invasion of RBCs *in vitro*. The modified iRBC surface triggered PS-CD36-mediated phagocytosis of iRBCs, host type I interferon (IFN-I) signaling, and T cell differentiation, leading to improved host survival. This study reveals a previously unknown role of PyEBL in regulating host-pathogen interaction and innate immune responses, which may be explored for developing disease control strategies.

**IMPORTANCE** Malaria is a deadly parasitic disease that continues to afflict hundreds of millions of people every year. Infections with malaria parasites can be asymptomatic, with mild symptoms, or fatal, depending on a delicate balance of host immune responses. Malaria parasites enter host red blood cells (RBCs) through interactions between parasite ligands and host receptors, such as erythrocyte-binding-like (EBL) proteins and host Duffy antigen receptor for chemokines (DARC). *Plasmodium yoelii* EBL (PyEBL) is known to play a role in parasite invasion of RBCs. Here, we show that PyEBL also affects disease severity through modulation of host immune responses,

**Citation** Peng Y-C, Qi Y, Zhang C, Yao X, Wu J, Pattaradilokrat S, Xia L, Tumas KC, He X, Ishizaki T, Qi C-F, Holder AA, Myers TG, Long CA, Kaneko O, Li J, Su X-Z. 2020. *Plasmodium yoelii* erythrocyte-binding-like protein modulates host cell membrane structure, immunity, and disease severity. mBio 11:e02995-19. <https://doi.org/10.1128/mBio.02995-19>.

**Editor** Stephen L. Hajduk, University of Georgia

This is a work of the U.S. Government and is not subject to copyright protection in the United States. Foreign copyrights may apply.

Address correspondence to Xin-zhuan Su, xsu@niaid.nih.gov.

This article is a direct contribution from Xin-zhuan Su, a Fellow of the American Academy of Microbiology, who arranged for and secured reviews by Sanjai Kumar, Food and Drug Administration, and Fidel Zavala, Johns Hopkins University.

**Received** 14 November 2019

**Accepted** 19 November 2019

**Published** 7 January 2020

particularly type I interferon (IFN-I) signaling. This discovery assigns a new function to PyEBL and provides a mechanism for developing disease control strategies.

**KEYWORDS** *Plasmodium*, mouse, erythrocyte-binding-like, EBL, interferon, pathogen-host interaction, phagocytosis

Erythrocyte-binding-like (EBL) proteins are a family of type I transmembrane proteins that localize to micronemes of a malaria merozoite and, following microneme discharge, play a crucial role during the invasion of red blood cells (RBCs) (1). An EBL protein generally has an N-terminal cysteine (Cys)-rich binding domain (region 2) and a C-terminal Cys-rich trafficking domain (C-Cys domain or region 6), along with a signal sequence and a transmembrane domain (1, 2). The N-terminal Cys-rich region consists of one or two Duffy-binding-like (DBL) domains that bind host proteins like the Duffy antigen receptor for chemokines (DARC) or glycophorin A on the erythrocyte surface during invasion of RBCs (3, 4). The C-terminal C-Cys domain directs the protein for microneme trafficking (5, 6). *Plasmodium yoelii* has one EBL gene (*Pyeb1*), encoding a protein (PyEBL) with a single DBL domain (1). A cysteine-to-arginine substitution at residue 713 (C713R) in the PyEBL C-Cys domain has been linked to parasite growth and virulence *in vivo* in the 17X lineage (7, 8). The parasite line 17XL (or YM) has the R713 variant C-Cys domain, grows fast, and kills its host by day 7, whereas the 17X (17XNL) line has the C713 variant, grows slowly, and is cured by the host (7, 8). The 17X, 17XL, 17XNL, and YM lines are isogenic parasites derived from a parasite isolated from a thick rat (9). In addition, EBL protein with C713 is localized in merozoite micronemes, whereas the R713 protein is mostly mistargeted to dense granules (DGs). Although these results suggest that PyEBL has a direct role in parasite invasion and virulence, it is difficult to explain the observation that abnormal localization of the variant PyEBL can greatly improve the parasite growth rate. Recently, PyEBL was found to be translocated to the merozoite surface as a confined patch in both the 17XL and 17XNL lines of *P. yoelii* (10), which may help maintain normal invasion of RBCs but cannot explain the enhanced growth rate of 17XL. The activation of other genes playing a role in invasion, such as those encoding Py235 rhoptry proteins, may help explain these paradoxical observations (8, 11, 12). Reticulocyte-binding-like (RBL) proteins (including Py235) can function cooperatively in the malaria parasite's invasion of human erythrocytes (13), and disruption of a Py235 gene affects parasite binding to RBCs (14). Another potential explanation for increased *in vivo* parasite growth after the C713R substitution is modulation of host immune responses that may differentially inhibit the growth of the parasites. In immunocompromised mice, the nonlethal, slowly growing 17XNL parasite grew fast and became lethal (15, 16), suggesting that host immunity plays a role in restricting parasite growth and virulence.

We previously performed genetic crosses between *Plasmodium yoelii nigeriensis* strain N67 and 17XNL parasites and found a significant linkage of a growth-related virulence phenotype to genetic loci on chromosomes 7, 10, and 13 (17). The chromosome 13 locus contains the gene encoding PyEBL, in which a Cys-to-Tyr substitution at residue 741 (C741Y) in the C-Cys domain was implicated in the differences of virulence between N67 and *P. yoellii nigeriensis* strain N67C parasite lines. N67C was originally named 33X(Pr3) and was deposited in MR4 under that name (MRA-754) by David Walliker, University of Edinburgh. Genotyping of 33X(Pr3), 33X, YM, 17XNL, and N67 parasite lines with microsatellites suggested that the 33X(Pr3) and N67 strains were closely related; therefore, 33X(Pr3) was renamed N67C (17). In contrast, 33X is genetically different from 33X(Pr3), N67, YM, and 17XL (17). In C57BL/6 mice, infection with N67C resulted in 40 to 50% parasitemia and host death on day 7 postinfection (p.i.), whereas mice infected with N67 suppressed the parasitemia to under 5% on day 7 p.i. (18). The suppression of N67 parasitemia was associated with N67 parasite stimulation of a strong early type I interferon (IFN-I) response (19). We hypothesize that parasites with the C741Y substitution trigger a unique immune response that in turn affects parasite growth.

In this study, we exchanged the C741 and Y741 alleles of PyEBL between N67 and N67C parasites and showed that allelic replacements altered parasite growth and virulence and host immune responses but not invasion of RBCs. Our study also reveals a previously unknown mechanism of host-parasite interaction mediated by PyEBL, showing increased phosphatidylserine (PS) exposure on infected RBCs (iRBCs), altered osmotic fragility, enhanced phagocytosis of iRBCs, an elevated IFN-I response, and improved parasitemia control after the C741Y substitution. This study demonstrates that a single amino acid substitution in a pathogen genome can result in major alterations in the host-parasite interface, with significant consequences for host viability, and provides a paradigm shift in our understanding of the roles of PyEBL in host-pathogen interaction during malarial-parasite infection.

## RESULTS

### Allelic exchange of C741Y alters parasite growth and disease severity *in vivo*.

To confirm functionally that the C741Y substitution plays a key role in control of parasitemia and parasite virulence, we constructed two linear DNA fragments to replace C741 with Y741 in N67C (N67C<sup>C-Y</sup>) parasites and Y741 with C741 in N67 (N67<sup>Y-C</sup>) parasites (Fig. S1A and B in the supplemental material). We also constructed synonymous controls, replacing C741 with C741 in N67C (N67C<sup>C-C</sup>) parasites and Y741 with Y741 in N67 (N67<sup>Y-Y</sup>) parasites. Integration and replacement of the amino acids at the genetic level were confirmed by PCR amplification (Fig. S1C and D) and DNA sequencing (Fig. S1E). After several rounds of transfection and cloning, we obtained 3 to 10 clones for each allelic replacement (Table S1).

The allele-exchanged and the parental N67 and N67C lines ( $1 \times 10^6$  parasites) were injected into 5 mice per group to evaluate parasitemia, host body weight, and mortality. Infection with N67C<sup>C-Y</sup> produced parasitemia curves, body weights, and survival rates similar to those of N67, whereas the phenotype of N67<sup>Y-C</sup> parasite infection was similar to that of N67C (Fig. 1A to C and Table S1). Synonymous substitution (N67<sup>Y-Y</sup> and N67C<sup>C-C</sup>) had no effect on parasite growth, body weight, or survival rate. Compared with mice infected with parasites carrying the C741 allele (N67C, N67<sup>Y-C</sup>, and N67C<sup>C-C</sup>), those infected with parasites carrying the Y741 allele (N67, N67<sup>Y-Y</sup>, and N67C<sup>C-Y</sup>) had significantly higher body weight ( $15.2 \pm 0.3$  g versus  $13.5 \pm 0.3$  g [mean  $\pm$  standard deviation];  $P < 0.001$ ; Mann Whitney test), lower parasitemia on day 7 p.i. ( $15.6\% \pm 2.5\%$  versus  $35.0\% \pm 1.1\%$ ;  $P < 0.001$ ), and longer survival ( $>14$  days versus 7 days), suggesting that the C741Y substitution indeed had a major impact on parasite growth and disease severity from day 5 onwards (Fig. 1A to C and Table S1).

### The C741Y substitution does not affect parasite invasion of RBCs *in vitro*.

To investigate whether the C741Y substitution affects parasite invasion of RBCs without the influence of host immunity, we used an *in vitro* invasion assay (20) and counted iRBCs 18 h after the addition of purified merozoites to RBCs (Fig. 1D). Similar invasion rates were observed for N67 and N67C (Fig. 1E), with the majority of the parasites being ring stage 18 h after the addition of merozoites (Fig. 1F). We also counted parasitemia at different time points. As expected, no significant difference in parasitemia levels was observed between the N67 and N67C cultures at 18 h, 24 h, and 40 h (Fig. 1G), because *P. yoelii* parasites cannot automatically release merozoites for reinvasion under the current culture conditions. A significant difference was observed at 48 h postinvasion; however, the difference in parasitemia levels was likely due to faster parasite loss for N67C, because parasitemia decreased over time. The percentages of schizonts also increased over time (Fig. 1H), suggesting normal growth of parasites once they were within RBCs. These results demonstrate that the C741Y substitution does not significantly change RBC invasion *in vitro*, which is consistent with the observations of similar *in vivo* parasitemia levels for C741 and Y741 parasites before day 5 p.i. (Fig. 1A). Therefore, the differences in parasitemia levels after day 5 p.i. and in disease phenotype are not due to a change in RBC invasion efficiency resulting from the C741Y substitution. Differential host immune responses caused by the C741Y substitution may play a role in the altered *in vivo* parasite growth and host survival rate.

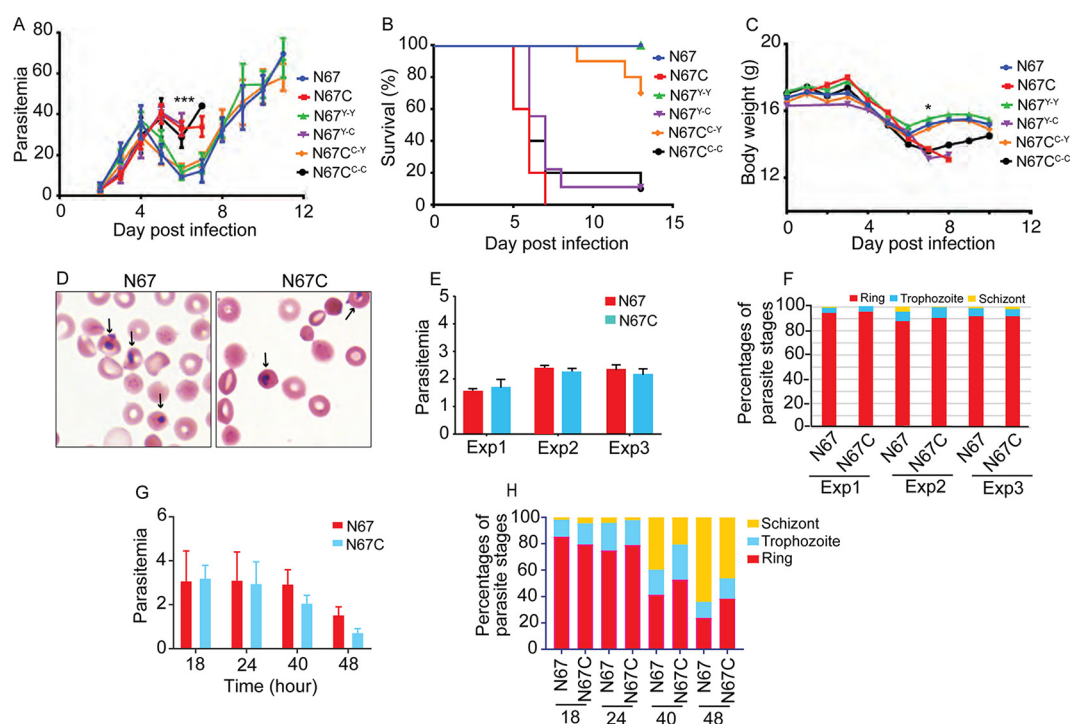


**FIG 1** *In vivo* and *in vitro* (invasion) parasite growth rates, host survival rates, and host body weights after infection with parasites carrying PyEBL C741 or Y741 allele. (A) Parasitemias of parental and allele-exchanged *P. yoelii* clones. (B) Mouse survival rates after infection with different parasite clones. (C) Body weights of mice infected with parasites as indicated. (A to C) Mean values + standard deviations (SD) from 5 mice in each group. One-way analysis of variance (ANOVA): \*,  $P < 0.05$ , and \*\*\*,  $P < 0.001$ , for all comparisons. (D) Smears of *in vitro* cultures with RBCs reinvaded by *P. yoelii* N67 or N67C parasites. (E) Parasitemias of N67 and N67C parasites 18 h after addition of purified merozoites to red blood cells. (F) Percentages of ring, trophozoite, and schizont stages 18 h after invasion. (G) Parasitemias over time after *in vitro* invasion of N67 and N67C merozoites. (H) Percentages of ring, trophozoite, and schizont stages at different time points after invasion. (E and G) Mean values + SD were plotted.

### C741Y substitution alters PyEBL protein trafficking in merozoites and iRBCs.

The C741Y substitution is located in the trafficking C-Cys domain (Fig. S1A) (6, 8), which may affect PyEBL protein expression and localization. To investigate PyEBL protein expression and localization, we performed an immunofluorescence assay (IFA) using anti-EBL antibodies (8, 10) and examined protein localization under a confocal microscope. The C741 PyEBL was expressed as a focused dot in merozoites (Fig. 2A and B), consistent with an apical location, whereas Y741 PyEBL was diffuse, with more than one dot (Fig. 2C and D). C741Y allelic replacement (N67C<sup>C-Y</sup>) (Fig. 2E) converted the single-dot expression pattern to one similar to that of N67 (Fig. 2C); however, the Y741C replacement in N67 (N67<sup>Y-C</sup>) (Fig. 2F) did not completely change the pattern to the single dots typically seen in N67C (Fig. 2A). These results suggest apical and DG localization for parasites with the Y741 allele, similar to those observed with *P. yoelii* 17XL with the C713R substitution in the C-Cys domain (8). Thus, the C741Y substitution changes PyEBL trafficking in the merozoite. We also found that PyEBL may be expressed in the cytoplasm of iRBCs (Fig. 2G to L) regardless of the amino acid at 741, although we cannot rule out nonspecific staining of other parasite proteins by the polyclonal antibodies.

To confirm the specificity of the anti-PyEBL antibodies and PyEBL expression in ring- and trophozoite-infected RBCs, we tagged PyEBL in N67 and N67C parasites with a hemagglutinin (HA)-Flag tag (HA::Flag) using a clustered regularly interspaced short palindromic repeat (CRISPR)–CRISPR-associated protein 9 (Cas9) method (Fig. S2A) (21). After transfection and drug selection, chromosomal integration of the sequence was confirmed using PCR (Fig. S2B and C). The high specificity of the anti-HA monoclonal antibody (3724; Cell Signaling) allowed detection of differential PyEBL expression in N67- and N67C-infected RBCs. Whereas an HA signal could be easily detected in



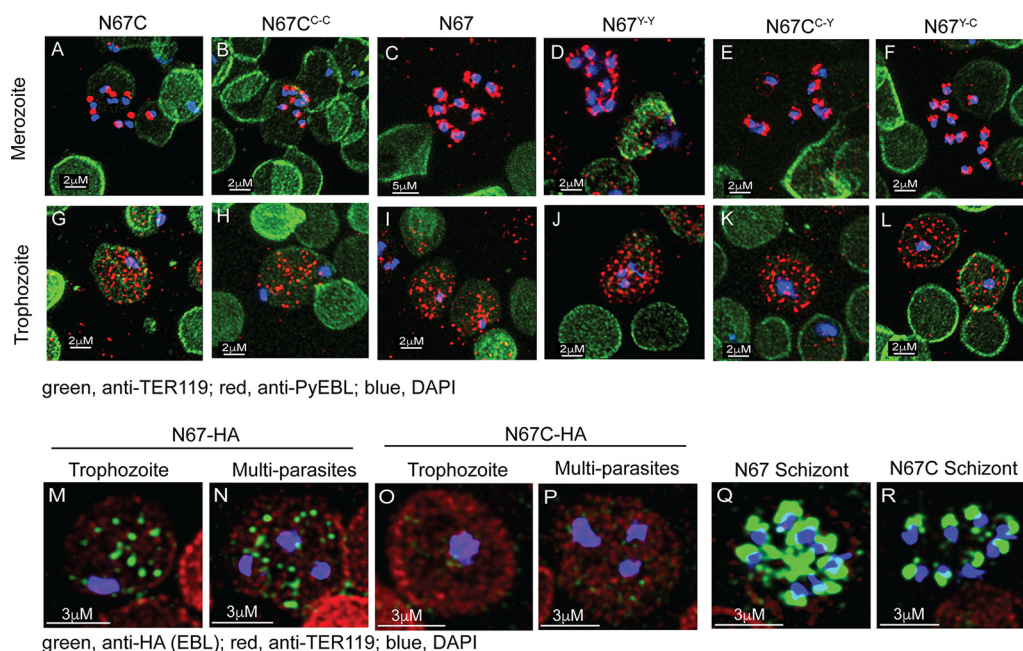
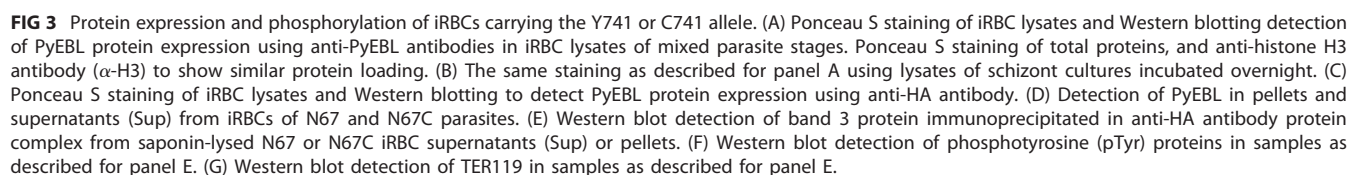


**FIG 2** PyEBL protein expression and localization in merozoites and infected red blood cells. (A to L) IFA was performed as described in Text S1. Red, anti-PyEBL antibody; blue, DAPI (4',6-diamidino-2-phenylindole); green, anti-TER119 antibody for red blood cell (RBC) membrane. (A to F) PyEBL expression in merozoites of N67, N67C, and allele-exchanged parasites as marked. (G to L) PyEBL expression in RBCs infected with ring or trophozoite stages. Note weak staining of iRBC membranes compared with those of uninfected RBCs. (M to R) Images from N67 and N67C parasites with HA::Flag-tagged EBL. Green, signals from anti-HA antibody; red, anti-TER119 antibody; blue, DAPI. (M and N) Membrane-bound vesicles (green dots) in the cytoplasm of red blood cells infected with a single parasite (M) or three N67 parasites (N). (O and P) Similar images from N67C-infected RBCs. (Q and R) Schizonts of N67 (Q) or N67C (R) parasites.

cytoplasmic punctate vesicles of iRBCs containing a single nucleus (ring or trophozoite stage) of the N67 parasite line (Fig. 2M and N), few green dots could be seen in N67C iRBCs (Fig. 2O and P). The anti-HA antibody also confirmed the diffuse staining and focused dot pattern in N67 (Fig. 2Q) and N67C (Fig. 2R) merozoites, respectively, supporting the idea that the C741Y substitution affects PyEBL trafficking in merozoites and iRBCs.

#### The C741Y substitution affects PyEBL processing and host band 3 distribution.

We used SDS-PAGE and Western blotting to investigate the expression and potential proteolytic processing of PyEBL. Anti-PyEBL polyclonal antibodies detected multiple bands of ~75 to 100 kDa, including one that was smaller in N67C parasite extracts (Fig. 3A, middle band indicated by red arrow), suggesting differential protein processing. Extracts from N67 and N67C<sup>C-Y</sup> parasites had the same band patterns, but the middle band in N67<sup>Y-C</sup> lysates was the same size as that of N67 lysates (did not change). The upper band disappeared from all lysates when the parasites were cultured overnight at 37°C (Fig. 3B), suggesting further processing. Interestingly, the N67<sup>Y-C</sup> lysate had doublet bands, with the top band the same size as that in N67 and the lower band similar to that of the N67C parasite (Fig. 3B, red arrow), which is consistent with the incompletely changed cellular phenotypes. We also used anti-HA antibody to detect HA-tagged PyEBL in N67 and N67C parasite lysates and showed a band that was slightly larger in N67 than in N67C lysates (Fig. 3C). To confirm the presence of the protein in iRBCs, we lysed iRBCs of all parasite stages with saponin (0.1%) and prepared supernatants and pellets after centrifugation ( $1,455 \times g$  at 4°C for 10 min). We then performed immunoprecipitation (IP) using anti-HA antibody to pull down HA-tagged PyEBL from the supernatants and solubilized pellets, respectively. PyEBL-HA was detected by anti-HA antibody from both supernatant and pellet fractions of both N67 and N67C iRBCs (Fig. 3D). The pulldown of PyEBL from the supernatants of iRBCs supports the observation by fluorescence microscopy of cytoplasmic/cytosolic expression of



To investigate potential PyEBL-host protein interactions, we first used Western blotting with anti-band 3 antibody to investigate whether band 3 was coprecipitated by anti-HA antibody. A major band 3 band was detected in the precipitates from supernatants, whereas three bands were detected in those of pellets, with the major band slightly smaller than that from supernatants (Fig. 3E). The middle band (and the band in supernatants) may have resulted from modifications like phosphorylation of the lower band, and the ~200-kDa band could be a dimer. Band 3 distribution in the supernatant and pellet precipitates was different between N67 and N67C parasites: the relative band 3 intensities (ratios) of pellet over supernatant were 5.52 for N67C iRBCs and 1.48 for N67 iRBCs, suggesting an increased cytosolic band 3 (or reduced membrane-bound form) in N67 iRBCs. If we consider the anti-HA signal to be a loading control (the same amounts of samples loaded) and divide the band 3 signal by the corresponding anti-HA signal, we obtain ratios of 3.1 for the N67C/N67 supernatant fraction and 3.3 for the N67C/N67 pellet fraction, i.e., approximately 3-fold reduced binding of N67 PyEBL to band 3.

Downloaded from <http://mbio.asm.org/> on January 23, 2020 at THE FRANCIS CRICK INSTITUTE

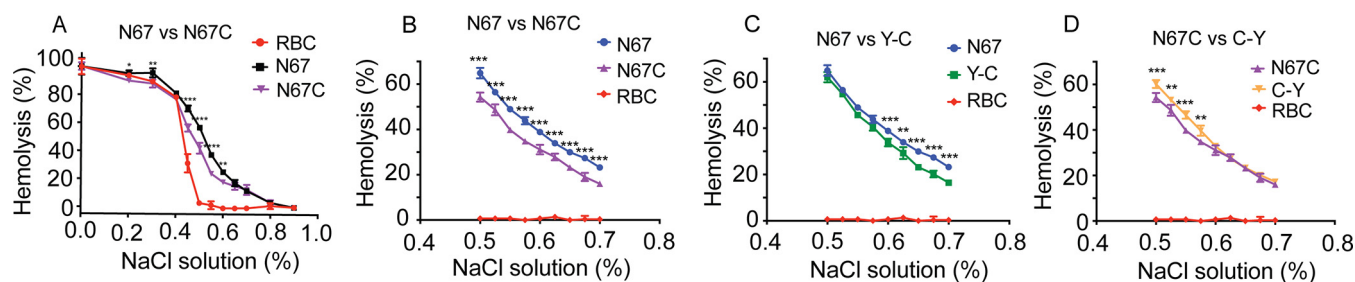


**FIG 4** Dynamics of osmotic lysis of RBCs and iRBCs carrying Y741 or C741 allele. (A) Dynamics of hemolysis of uninfected RBCs (uRBCs) and RBCs infected with N67 and N67C schizonts in different NaCl concentrations (0, 0.2, 0.3, 0.4, 0.5, 0.6, 0.7, 0.8, and 0.9%). (B) The same experiments described for panel A using NaCl concentrations from 0.5% to 0.7% (0.5, 0.525, 0.55, 0.575, 0.6, 0.625, 0.65, 0.675, and 0.7%). (C and D) The same experiments as described for panel B comparing N67 and N67<sup>Y-C</sup> (C) and N67C and N67C<sup>C-Y</sup> (D) parasites. Experiments were repeated independently (different mice at different times) at least twice. Mean values and SD are from 3 to 5 measurements. Two-way ANOVA: \*,  $P < 0.05$ ; \*\*,  $P < 0.01$ ; \*\*\*,  $P < 0.001$ .

bands of a similar size (Fig. 3G). Therefore, the C741Y substitution alters the relative band 3 distribution, increasing phosphorylated cytosolic band 3 (and possibly TER119) and reducing membrane-bound band 3 on iRBCs, which may affect cell membrane physiology. In summary, the C741Y substitution increases the relative amounts of cytosolic PyEBL and phosphorylated band 3 and reduces PyEBL-band 3 binding by approximately 3-fold, which may alter the membrane structure and physiology of iRBCs.

**The C741Y substitution increases iRBC osmotic fragility.** We next performed osmotic lysis experiments to evaluate the fragility of the iRBC membrane at different NaCl concentrations. Enriched schizonts were treated with different NaCl concentrations (0 to 1.0% [wt/vol]) and centrifuged immediately to pellet intact cells. The hemoglobin released into the supernatant was measured by absorbance at 540 nm. Both N67- and N67C-infected RBCs were lysed by NaCl concentrations significantly higher (Tukey's range test,  $P < 0.05$ ) than those required for uninfected RBCs (uRBCs), at NaCl concentrations ranging from 0.4% to 0.7% (Fig. 4A). iRBCs with N67 schizonts were also more fragile than those with N67C schizonts (the N67 curve is above the N67C curve), with significant differences in cell lysis at between 0.5% and 0.6% NaCl. We repeated the experiments focusing on salt concentrations between 0.5% and 0.7%. N67 schizont-infected cells were again significantly more sensitive to lysis than those containing N67C schizonts in the 0.5% to 0.7% salt concentration range (Fig. 4B). Interestingly, iRBCs infected with the N67<sup>Y-C</sup> parasite were significantly more resistant to lysis than those containing N67 parasites at higher salt concentrations (0.6% to 0.7%), whereas iRBCs containing N67C<sup>C-Y</sup> became significantly more sensitive to lysis than cells with N67C at lower salt concentrations (0.5% to 0.575%) (Fig. 4C and D). These results show that the C741Y substitution not only changes protein trafficking but also affects the membrane structure and osmotic fragility of iRBCs. Loss of red cell membrane integrity, such as the redistribution of membrane proteins and phospholipids (see below), could contribute to the differential hemolysis of RBCs (24, 25). These changes to iRBCs may also influence host cell recognition of iRBCs, the immune response, and disease pathology.

**The C741Y substitution changes host spleen pathology and production of cytokines/chemokines.** We next investigated pathological changes in the spleen and lung due to parasite infection. Hematoxylin and eosin (H&E) staining of spleens infected with N67, N67C, N67<sup>Y-C</sup>, and N67C<sup>C-Y</sup> revealed splenomegaly in N67-infected mice and massive cell loss in N67C-infected mice at day 4 p.i. compared with the spleens of uninfected mice (Fig. 5A to F). Interestingly, the C741Y replacement (N67C<sup>C-Y</sup>) reduced the degree of cell loss and led to the splenomegaly that was associated with N67 (Y741) infection, although some small white spaces with parasite pigment were still evident at day 4 p.i. (Fig. 5G and H). Conversely, Y741C replacement (N67<sup>Y-C</sup>) increased cell loss compared with that in spleens of mice infected with N67 but without reduction in spleen size (Fig. 5I and J). Additionally, more Ly6G<sup>+</sup> cells (monocytes, granulocytes, and



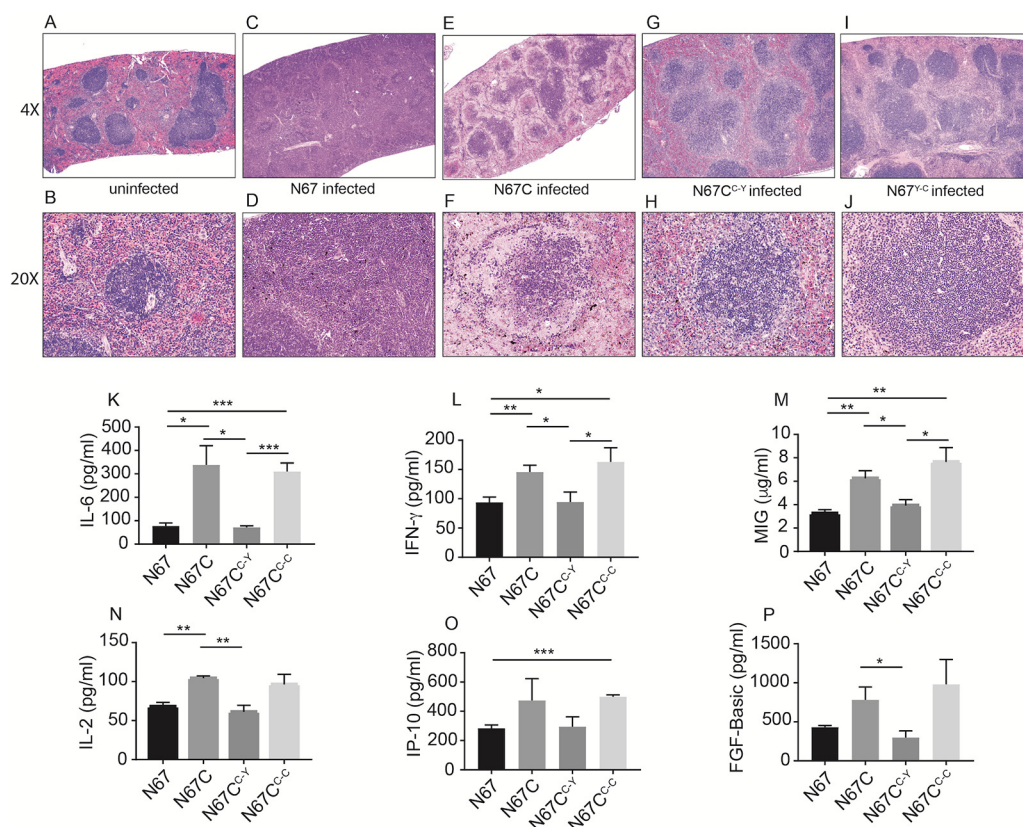


**FIG 5** Spleen pathology and serum cytokine/chemokine levels after infection with parasites carrying C741 or Y741 allele. (A to J) Images of H&E-stained spleen tissues from mice infected with different allele-exchanged parasite clones, magnified at 4× (A, C, E, G, and I) and 20× (B, D, F, H, and J). (K to P) Cytokine/chemokine levels in mice infected with parasites with either the C741 or Y741 allele on day 4 postinfection. Cytokines/chemokines in plasma collected from mice infected with N67, N67C, N67C<sup>C-Y</sup>, and N67C<sup>C-C</sup> parasites on day 4 postinfection were measured using a bead array (Bio-Rad). Mean values and standard errors of the means (SEM) from 4 or 5 mice. One-way ANOVA: \*,  $P < 0.05$ ; \*\*,  $P < 0.01$ ; \*\*\*,  $P < 0.001$ .

neutrophils) were detected in the spleens and lungs of mice infected with Y741 parasites than in those of mice infected with C741 parasites (Fig. S3A to Q and Table S1). These results show that the C741Y substitution affects host response and tissue pathology, although the reversal of phenotype following allelic exchange was not complete, which suggests contributions from other parasite genes.

We measured the serum levels of some cytokines/chemokines on day 4 p.i. and found that mice infected with N67C or N67C<sup>C-C</sup> had significantly higher levels of interleukin-6 (IL-6), gamma interferon (IFN-γ), and monokine induced by IFN-γ (MIG) than those infected with N67 or N67C<sup>C-Y</sup> on day 4 p.i. (Fig. 5K to M). The levels of IL-2, IFN-γ-induced protein 10 (IP-10), and basic fibroblast growth factor (FGF-basic) were also higher in mice infected with parasites carrying the C741 allele than in those carrying the Y741 allele, although not all the comparisons were significant (Fig. 5N to P). These data suggest stronger inflammatory responses in mice infected with parasites carrying the C741 allele than in those carrying the Y741 allele at day 4 p.i., resulting in early cell and host death. Together, the similar early *in vivo* parasitemias and *in vitro* invasion rates, differential levels of protein expression in iRBCs, altered spleen pathology, changes in serum levels of cytokines/chemokines, and longer host survival rates suggest that the C741Y substitution in PyEBL mainly affects host immune responses, not RBC invasion, that in turn shape parasite growth and host pathology and survival.

**Y741 linked to elevated IFN-I response, isotype switching, and T-helper cell differentiation.** To systematically investigate the molecular mechanisms underlying the differential immune responses and disease phenotypes caused by parasites with either C741 or Y741 variants, we performed transcriptome sequencing (RNA-seq)



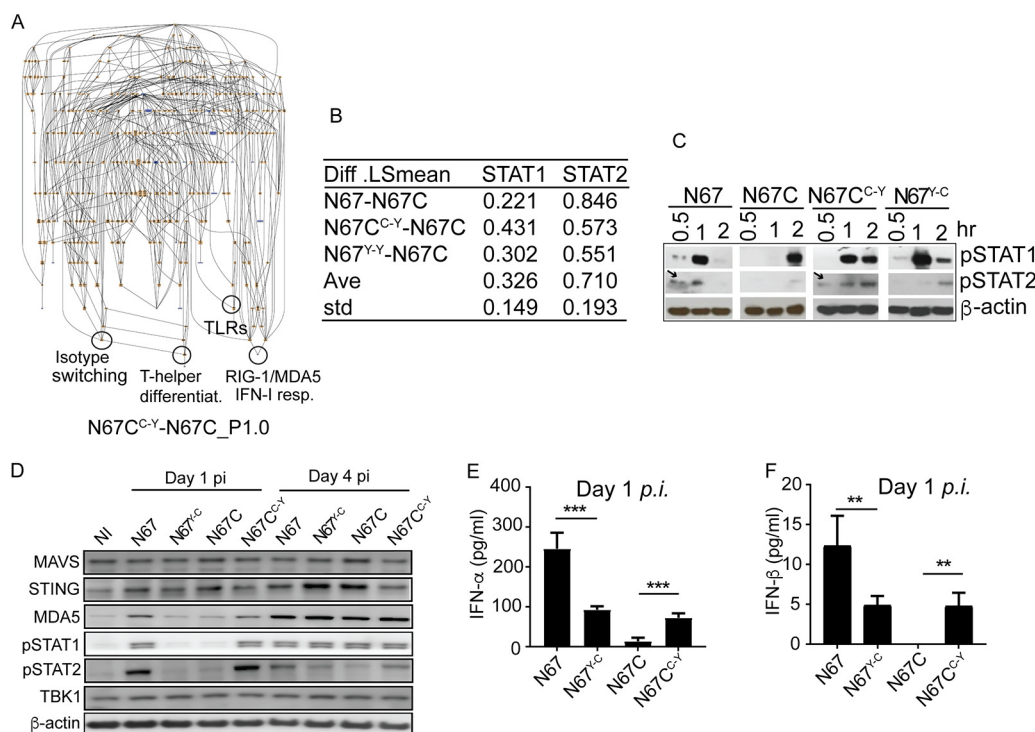


**FIG 6** PyEBL Y741 allele is associated with elevated type I interferon response, differentiation of T-helper cells, and Ig isotype switching. (A) Enriched biological process ontologies from differentially expressed genes in spleens of mice infected with parasites containing the Y741 (N67C<sup>C-Y</sup>) or C741 (N67C) allele. Lists of differentially expressed genes with a cutoff at  $\log_2(\text{norm.reads } x / \text{norm.reads } y) \geq 1$  of normalized reads per kilobase per million (RPKM) were uploaded onto Gene Ontology (GO) tools (<http://geneontology.org/page/go-enrichment-analysis>), and search results in GO tree view images from the website are presented. Enriched terms are for genes expressed at higher levels in N67C<sup>C-Y</sup>-infected mice than in N67C-infected mice. differentiat., differentiation; resp., response. (B) Mice infected with parasites carrying the Y741 allele express consistently higher levels of *Stat1* (*t* test,  $P = 0.045$ ) and *Stat2* ( $P = 0.002$ ) transcripts from RNA-seq. Diff.LSmean, differences in least-squares means. (C) Protein phosphorylation detected by Western blotting using anti-pSTAT1 and anti-pSTAT2 antibodies. Bone marrow-derived macrophages (BMDMs) were incubated with red blood cells infected with parasites having the Y741 (N67 and N67C<sup>C-Y</sup>) or C741 (N67C and N67<sup>Y-C</sup>) allele for the indicated times. β-Actin is included as a protein loading control. (D) Western blotting of spleen lysates on days 1 and 4 postinfection with parasites as indicated. Proteins were detected using antibodies as indicated on the left side of the gels. β-Actin is included as a protein loading control. (E) Levels of IFN-α in the blood of mice infected with N67, N67C, N67<sup>Y-C</sup>, and N67C<sup>C-Y</sup> parasites on day 1 postinfection. (F) Levels of IFN-β in the blood of mice infected with N67, N67C, N67<sup>Y-C</sup>, and N67C<sup>C-Y</sup> parasites on day 1 postinfection. For panels E and F, mean values and SEM are from 3 to 5 replicates. Mann-Whitney U test: \*\*,  $P < 0.01$ ; \*\*\*,  $P < 0.001$ .

analysis of mRNA samples isolated from peripheral blood cells of mice infected with N67, N67C, N67<sup>Y-C</sup>, N67C<sup>C-Y</sup>, N67<sup>Y-Y</sup>, or N67C<sup>C-C</sup> parasites at day 4 p.i. (<https://www.ncbi.nlm.nih.gov/geo/query/acc.cgi?acc=GSE132796>). We compared host gene expression levels by counting reads per kilobase of transcript (RPKM) during infection with the parasite clones, using a cutoff value of  $[\log_2(\text{RPKM}) \text{ ratio}] \geq 1.0$  (or ~2.7-fold difference) (Table S2A). We then performed GO term enrichment analysis on the lists of genes differentially expressed between the two parasite groups using Gene Ontology (GO) tools (<http://go.princeton.edu>). Parasites having the Y741 PyEBL stimulated stronger immune responses (false discovery rate [FDR],  $q < 0.01$ ), particularly in IFN-I (retinoic acid-inducible gene I [RIG-I]/melanoma differentiation-associated gene 5 [MDR5] and Toll-like receptor [TLR]) signaling pathways, T-helper cell differentiation, and IgG isotype switching, than parasites with the C741 variant (Fig. 6A; Table S2B and Fig. S3P and Q), which may explain the better control of parasitemia and better host survival for infections with Y741 parasites. Some of the genes playing a role in these pathways include *Ercc1* in DNA repair and recombination, *Xcl1*, *Prkcz*, and *Rsad2* in positive regulation of Th2 cell cytokine production, and *Lcn2*, *Isg20*, *Oas1*, *Oas2*, *Oasl2*, *Clenc4n*, *Mx2*, *Tlr2*, *Tlr5*, *Tlr12*, *Ifit1*, etc., in innate and IFN-I responses. We also performed upstream regulator analysis on genes differentially expressed in mice infected with

parasites carrying C741 or Y741 variants using Ingenuity Pathway Analysis (IPA; Qiagen, Inc.). Comparison of the differentially expressed genes from mice infected with N67C<sup>C-Y</sup> and N67C showed significantly higher scores for upstream regulator activation of elements in the IFN-I signaling pathway, such as IFN regulatory factor 3 (IRF3), IRF7, STAT1, STAT2, TLR3, TLR9, IFNB1 (IFN- $\beta$ 1), mitochondrial antiviral signaling protein (MAVS), DDX58 (RIG-I), and cyclic GMP-AMP synthase (cGAS) in mice infected with N67C<sup>C-Y</sup> parasites (Table S3A). These results are consistent with the outcome of the GO term analysis, showing activation of IFN-I responses in mice infected with Y741 parasites.

We compared the transcription levels of *stat1* and *stat2* genes that are critical in interferon production and found higher mRNA levels for both genes in the spleens of mice infected with parasites carrying Y741 than in spleens of mice infected with parasites carrying C741 (Fig. 6B). Consistently, higher levels of STAT2 phosphorylation (pSTAT2) were detected in bone marrow-derived macrophages (BMDMs) 30 min to 1 h after incubation with iRBCs carrying Y741 parasites than after incubation with iRBCs carrying C741 parasites (Fig. 6C, arrows), and high levels of pSTAT1 were detected in both Y741 and C741 groups after 1 to 2 h of incubation (Fig. 6C). Higher levels of pSTAT1, pSTAT2 and MDA5, but not stimulator of interferon genes (STING), MAVS, or TANK-binding kinase 1 (TBK1), were also detected in the spleens of mice infected with Y741 parasites on day 1 p.i. (Fig. 6D). Except for pSTAT2 and STING, no differences were observed for any of the molecules at day 4 p.i. Additionally, serum IFN- $\alpha$  and IFN- $\beta$  levels were significantly higher in mice infected with Y741 parasites following allelic replacement (Fig. 6E and F). These data demonstrate that parasites carrying the Y741 variant induce a stronger early IFN-I response than those with C741.

The RNA-seq analysis also allowed simultaneous monitoring of parasite gene expression. Only 40 differentially expressed (up or down) genes were identified, including genes encoding Py235 (Table S3B and Text S1). However, indirect immunofluorescence assay (IFA) of specific Py235 protein expression revealed no differences in the levels or patterns of protein expression (Fig. S4 and Text S1). The role of Py235 in the observed differences in parasite growth, host responses, and disease pathology requires further investigation.

**Y741 iRBCs trigger strong PS-CD36-mediated phagocytosis.** Because iRBCs lack intracellular pathogen-sensing machinery, recognition of parasite patterns like RNA/DNA to induce IFN-I signaling or T cell activation likely requires digestion of iRBCs by antigen-presenting cells (26). Phosphatidylserine (PS) exposure at the outer membrane leaflet of the RBC is one of the characteristics of eryptosis that can be triggered by various factors, including malaria infection (27–29). Therefore, we analyzed the *in vitro* phagocytosis of RBCs infected with N67, N67C, and allele-exchanged parasites to evaluate both phagocytosis and PS exposure on iRBCs. Results from the assay using bone marrow-derived dendritic cells (BMDCs) showed that RBCs infected with Y741 parasites could stimulate significantly higher levels of phagocytosis than those infected with C741 parasites (Fig. 7A and B). Similar results were obtained using BMDMs (Fig. 7C and D).

To investigate the mechanism that may contribute to the differential phagocytosis, we stained iRBCs with annexin V, which binds to PS on the cell surface, and showed that RBCs infected with Y741 parasites had significantly more annexin V binding than those infected with C741 parasites (Fig. 7E). These results suggest that the C741Y substitution causes increased surface PS exposure on iRBCs, which triggers a strong phagocytic response. Many receptors on host cell surfaces can recognize target cell molecules; for example, CD36 is known to recognize oxidized patterns and PS on apoptotic cells (30, 31), including PS exposed on *Plasmodium falciparum*-infected RBCs (29). We next used antibodies against CD36, DARC (a putative receptor for PyEBL), and annexin V to block potential interactions between iRBCs and dendritic cells (DCs). Only anti-CD36 antibody could significantly inhibit phagocytosis in the presence or absence of anti-CD16/CD32

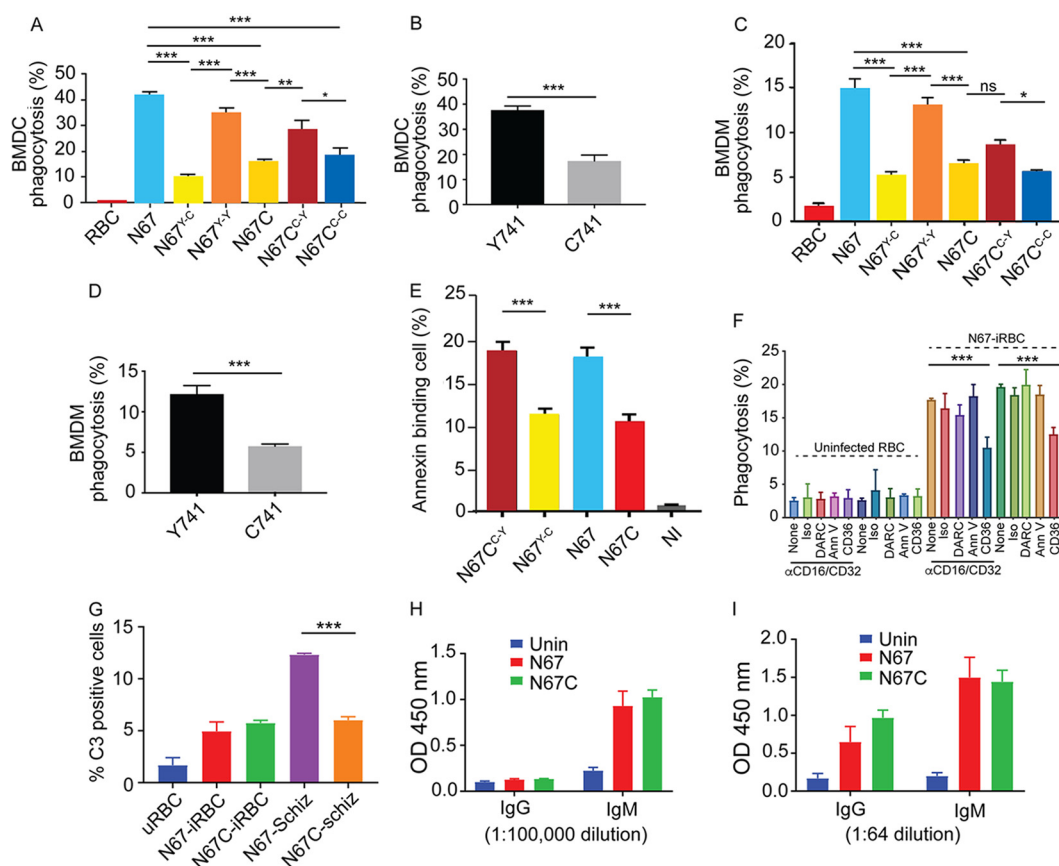


**FIG 7** PyEBL Y741 allele is associated with increased annexin V binding and PS-CD36-mediated phagocytosis. (A) Percentages of RBCs infected with individual parasite lines carrying the Y741 or C741 allele phagocytized by bone marrow-derived dendritic cells (BMDcs). (B) Mean percentages of phagocytized iRBCs from C741 or Y741 parasite groups. (C and D) The same experiments as described for panels A and B but performed using bone marrow-derived macrophages (BMDMs). (E) Percentages of iRBCs bound by annexin V. RBCs infected with different parasites are as marked. NI, noninfected RBCs. (F) Percentages of phagocytized RBCs or iRBCs with or without blocking antibodies. Anti-CD16/CD32 antibodies were added to block nonspecific binding through CD16/CD32. Iso, isotype antibody control. (G) Percentages of red blood cells infected with N67 or N67C schizonts stained by anti-complement 3 (C3) antibody and counted using flow cytometry. (H) Serum levels of IgG and IgM in uninfected mice (Unin) and mice infected with N67 or N67C on day 6 postinfection, measured using ELISA with 1:100,000 antibody dilution. OD, optical density. (I) The same measurements as described for panel G but using plates coated with *P. yoelii* parasite lysates (1:64 dilution). Mean values and SD are from 3 to 5 replicates. ANOVA and Mann Whitney (B and D) tests: \*,  $P < 0.05$ ; \*\*,  $P < 0.01$ ; \*\*\*,  $P < 0.001$ .

antibodies that block nonspecific Fc $\gamma$  receptor III (Fc $\gamma$ RIII) and Fc $\gamma$ RII binding to IgG (32) (Fig. 7F). The results suggest that PS-CD36 interaction mediates phagocytosis of iRBCs and triggers a strong IFN-I response, which helps suppress the parasitemia after day 4 p.i. We also investigated the possibility of altered complement binding after the C741Y substitution. Anti-C3 antibody staining showed a significantly higher percentage of anti-C3 antibody binding to N67 schizont-infected RBCs than to N67C schizont-infected RBCs (Fig. 7G). The result suggests that the C741Y substitution may change the susceptibility of iRBCs to complement pathways.

Our RNA-seq data indicate that the C741Y substitution affects the expression of selected genes playing a role in antibody isotype switch (Fig. 6A). We next measured IgG and IgM levels in the blood of mice infected with N67 or N67C, respectively, using enzyme-linked immunosorbent assay (ELISA). No significant differences in IgG and IgM levels were observed, either in the levels of total or parasite-specific antibodies, between N67- and N67C-infected mice at day 6 p.i. (Fig. 7H and I). The lack of any difference in antibody levels is likely due to blood collection at early infection, before the host can mount an effective IgG response.

## DISCUSSION

Previous studies on EBL proteins in malaria parasites have focused on their roles in RBC invasion (1, 33–35). Our present study shows that PyEBL also modulates host recognition of iRBCs and immune responses through interaction with RBC membrane molecules, such as band 3 and PS, demonstrating a previously unrecognized mechanism of host-parasite interaction mediated by PyEBL (Fig. S5 in the supplemental material). We show that a single C741Y amino acid substitution in the C-Cys domain of PyEBL affects parasite growth and host survival, but not RBC invasion, through modification of the iRBC surface and host immunity. Mechanistically, the C741Y substitution alters the iRBC membrane by increasing the number of PS molecules on the surface and reducing membrane-bound band 3 after phosphorylation. iRBC membrane modifications increase membrane fragility and trigger phagocytosis mediated through the interaction of PS and CD36 (and potentially other molecules). Elevated levels of phagocytosis may release more parasite materials, such as DNA/RNA, to stimulate IFN- $\gamma$  production, which can modulate T cell responses and antibody production (36, 37), resulting in reduced inflammation and a better host survival rate. This discovery adds a new function to PyEBL and places it with a group of *Plasmodium* molecules, such as *Plasmodium falciparum* erythrocyte membrane protein (PfEMP1), which also have DBL domains, encoded by the variant (*var*) genes that have been shown to modulate host immune response and pathogenesis (38–40).

Neither of the PyEBL allelic exchanges (N67<sup>Y-C</sup> and N67C<sup>C-Y</sup>) completely changed the phenotypes of the IFA staining pattern in merozoites, spleen tissue pathology, serum IFN- $\gamma$  level after infection, phagocytosis, or osmotic lysis to the levels of those of wild-type parasites (N67 or N67C), suggesting that additional molecules contribute to these phenotypes. Although the replacement of Cys with Tyr in N67C (N67C<sup>C-Y</sup>) completely changed the PyEBL Western blot band pattern to a match for that of N67, the Y-to-C replacement in N67<sup>Y-C</sup> produced a partial change, with bands characteristic of both N67 and N67C present in the lysates from overnight-cultured schizonts (Fig. 3A). This incomplete protein processing is consistent with the partial reversal of other phenotypes in the N67<sup>Y-C</sup> parasite. The Western blot results also suggest that PyEBL is cleaved during parasite development from the ring/trophozoite to the schizont stage, at least in *in vitro* culture, because the top band disappears from samples of parasites cultured overnight. Additionally, the PyEBL is further cleaved to a smaller size more efficiently in N67C than in N67 parasites, which could contribute to the stronger binding to band 3 in the pulldown experiment. The ~78-kDa protein band may be a product of further PyEBL processing or another parasite protein cross-reacting with the rabbit anti-PyEBL polyclonal antibodies. Such cross-reactivity may generate nonspecific IFA staining and bring into question the cytoplasmic punctate staining in RBCs infected with ring/trophozoites. However, the similar staining of HA-tagged parasites by anti-HA antibody and the detection of PyEBL in the supernatants of saponin-lysed iRBCs confirm the presence of PyEBL in the cytoplasm of iRBCs.

Several lines of evidence suggest that the C741Y substitution changes iRBC cell surface molecule expression and/or composition: (i) increased osmotic fragility of Y741 iRBCs, likely due to changed expression and/or distribution of membrane transporters like band 3; (ii) elevated PS exposure on Y741 iRBCs, related to modification of the iRBC surface; and (iii) less efficient coprecipitation of band 3 by anti-HA antibody from membrane fractions of N67 iRBCs than from membrane fractions of N67C iRBCs, suggesting a differential interaction of PyEBL with band 3. A differential conformational change of band 3 in human erythrocytes after infection with two *P. falciparum* lines (FCR-3 and CS2), by an unknown mechanism, was reported previously (41). *P. falciparum* infection can induce hemichrome formation, oxidative aggregation of band 3, membrane deposition of complement and antibodies, and phagocytosis of iRBCs (42). Our observation of a PyEBL-band 3 interaction provides a possible explanation of the altered band 3 conformation. Band 3 was pulled down from both supernatants and pellets, suggesting that it is closely associated with PyEBL. However, although band 3



was coprecipitated by anti-HA antibody, PyEBL and band 3 may or may not interact directly. For example, band 3 and glycophorin A are components of the ankyrin complex (43), and TER119 is another protein associated with glycophorin A (44). Tyrosine phosphorylation of band 3 promotes its dissociation from the spectrin-actin skeleton (22), and tyrosine phosphorylation of band 3 (as well as band 4.2, catalase, and actin) has been reported after *P. falciparum* infection (23). It is possible that infection with Y741 parasites could change the phosphorylation of band 3 and other proteins and affect their presence on the iRBC membrane. Band 3 has also been reported to be a receptor for merozoite surface protein-1 and -9 (MSP1 and MSP 9) binding during *P. falciparum* invasion of erythrocytes (45, 46). The target of PyEBL binding, the mechanism of how C741Y substitution changes iRBC membrane structure, and whether *P. yoelii* infections differentially affect band 3 phosphorylation remain to be elucidated.

IFA and confocal microscopy analyses showed diffused PyEBL expression in Y741 merozoites and a focused dot in C741 merozoites (mostly two dots in N67<sup>Y-C</sup>, or partial reversal), similar to those observed in 17XL and 17XNL parasites (8), suggesting that some Y741 PyEBL protein may traffic to dense granules (DGs) in merozoites. A recent study showed that PyEBL of the 17XL line is translocated to the merozoite surface after parasite egress from the iRBC, despite its intracellular localization to DGs (10). Ring-infected erythrocyte surface antigen (RESA) is another DG protein that is translocated to the iRBC membrane, where it binds to spectrin (47, 48). R713 or Y741 PyEBL can still be translocated to the merozoite surface for invasion of RBCs, and because the substitution is not in receptor binding domain II (R2), amino acid changes in the C-Cys domain should not significantly affect RBC invasion, as confirmed in our *in vitro* invasion assays. Interestingly, 17X (17XNL) iRBCs were shown to induce a spleen blood barrier of fibroblastic origin and to adhere to the fibroblastic cells more strongly than 17XL iRBCs, which could be a mechanism for escaping macrophage clearance (49). These observations are consistent with our results showing that the parasites with C741 and Y741 have different surfaces, which may lead to differences in parasite binding to host cells, host immune responses, and spleen pathology.

A number of observations suggest that there is a higher IFN-I response in mice infected with Y741 parasites than in those infected with C741 parasites. The increased early STAT2 phosphorylation after incubation of Y741 iRBCs with BMDMs *in vitro*, the higher levels of MDA5 expression and phosphorylation of STAT1/STAT2 in the spleen, the elevated serum IFN- $\alpha/\beta$  levels, and the activation of upstream regulators in IFN-I pathways after infection with Y741 parasites all support this suggestion. Elevated phagocytosis of Y741 iRBCs by DC cells and/or macrophages may release parasite RNA/DNA into the cell cytoplasm or into the circulation and stimulate IFN-I production through cGAS/STING, RIG-I/MDA5/MAVS, or TRIF-mediated signaling pathways. However, we do not have direct evidence of released parasite RNA/DNA triggering IFN-I responses yet. Early production of IFN-I by the MAR5 pathway helps control parasitemia in N67-infected mice (18, 50), and here, we showed that spleen lysates from mice infected with N67 and N67C<sup>C-Y</sup> parasites contained higher levels of MDA5 on day 1 p.i. MDA5 recognition of parasite RNA may be the main pathway in the IFN-I response. In addition, the RNA-seq and GO term analyses suggest increased T-cell activation, including positive regulation of Th2 cell differentiation, and Ig isotype switching as early as day 4 p.i. in mice infected with Y741 parasites. These immune mechanisms may play a critical role in the decline of parasitemia at day 7 and the longer survival of mice infected with Y741 parasites than of those infected with C741 parasites. Together, our study shows that significant consequences in disease severity can occur with a single amino acid substitution in a pathogen genome and that PyEBL protein not only contributes to invasion of RBCs but can also affect host cell membrane structure and immunity. The discovery provides a paradigm shift in our understanding of PyEBL function and host-pathogen interaction during malarial-parasite infection.

## MATERIALS AND METHODS

**Ethics statement.** All animal procedures for this study were performed in accordance with the protocol approved (approval number LMVR11E) by the Institutional Animal Care and Use Committee (IACUC) at the National Institute of Allergy and Infectious Diseases (NIAID) following the guidelines of the Public Health Service Policy on Humane Care and Use of Laboratory Animals and AAALAC. All mice were maintained under pathogen-free conditions.

**Parasites, mice, and infection of mice.** N67 and N67C parasites and the procedures for infecting mice with the parasites were as described previously (17, 19). Parasites were thawed from frozen stocks and injected into naive C57BL/6 mice to initiate infection. An inoculum containing  $10^6$  iRBCs from the donor mice, suspended in 100  $\mu$ l phosphate-buffered saline (PBS), pH 7.4, was injected intravenously into experimental mice ( $n = 3$  to 6 mice per clone or strain). Inbred female C57BL/6 mice, aged 6 to 8 weeks old, were obtained from Charles River Laboratory, Jackson Laboratory, or NIAID/Taconic Repository, NIH. Parasitemia was monitored by microscopic examination of Giemsa-stained thin tail blood smears. Additional methods can be found in the supplemental materials (S1–S3).

**Data availability.** RNA-seq data were deposited in GenBank under GEO Series accession number GSE132796.

## SUPPLEMENTAL MATERIAL

Supplemental material is available online only.

**TEXT S1**, DOCX file, 0.05 MB.

**FIG S1**, TIF file, 0.9 MB.

**FIG S2**, TIF file, 0.3 MB.

**FIG S3**, TIF file, 15.9 MB.

**FIG S4**, TIF file, 1.7 MB.

**FIG S5**, TIF file, 1.3 MB.

**TABLE S1**, DOCX file, 0.01 MB.

**TABLE S2**, XLSX file, 7 MB.

**TABLE S3**, XLSX file, 0.1 MB.

**TABLE S4**, XLSX file, 0.01 MB.

## ACKNOWLEDGMENTS

This work was supported by the Division of Intramural Research, National Institute of Allergy and Infectious Diseases (NIAID), National Institutes of Health (NIH), USA. A.A.H. was supported by the Francis Crick Institute, which receives its core funding from Cancer Research UK (grant number FC001097), the UK Medical Research Council (grant number FC001097), and the Wellcome Trust (grant number FC001097). This work was also supported in part by Grant-in-Aid for Scientific Research number 16H05184 (O.K.), MEXT, Japan. T.I. is a recipient of the Japanese Society of Promotion Sciences (JSPS) DC1 scholarship. A part of this work was conducted at the Joint Usage/Research Center on Tropical Disease, Institute of Tropical Medicine, Nagasaki University, Japan. Y.Q., L.X., and J.L. were partially supported by China Scholarship Council.

We thank James M. Burns for the blood-stage antigens from *P. yoelii* 17XL and Bradley Otterson of the NIH library for editing.

Y.-C.P., Y.Q., C.Z., X.Y., J.W., L.X., K.C.T., X.H., T.I., C.-F.Q., and T.G.M. conducted the experiments and/or data analysis; A.A.H., O.K., and C.A.L. provided reagents and instructions and wrote the manuscript; J.L. and X.-Z.S. supervised the research; and X.-Z.S. designed the experiments and manuscript writing.

The authors declare no competing interests.

## REFERENCES

- Culleton R, Kaneko O. 2010. Erythrocyte binding ligands in malaria parasites: intracellular trafficking and parasite virulence. *Acta Trop* 114: 131–137. <https://doi.org/10.1016/j.actatropica.2009.10.025>.
- Prasad CD, Prasad Singh A, Chitnis CE, Sharma A. 2003. A *Plasmodium yoelii* erythrocyte binding protein that uses Duffy binding-like domain for invasion: a rodent model for studying erythrocyte invasion. *Mol Biochem Parasitol* 128:101–105. [https://doi.org/10.1016/s0166-6851\(03\)00040-9](https://doi.org/10.1016/s0166-6851(03)00040-9).
- Horuk R, Chitnis CE, Darbonne WC, Colby TJ, Rybicki A, Hadley TJ, Miller LH. 1993. A receptor for the malarial parasite *Plasmodium vivax*: the erythrocyte chemokine receptor. *Science* 261:1182–1184. <https://doi.org/10.1126/science.7689250>.
- Swardson-Oliver CJ, Dawson TC, Burnett RC, Peiper SC, Maeda N, Avery AC. 2002. *Plasmodium yoelii* uses the murine Duffy antigen receptor for chemokines as a receptor for normocyte invasion and an alternative receptor for reticulocyte invasion. *Blood* 99:2677–2684. <https://doi.org/10.1182/blood.v99.8.2677>.
- Adams JH, Hudson DE, Torii M, Ward GE, Wellemes TE, Aikawa M, Miller LH. 1990. The Duffy receptor family of *Plasmodium knowlesi* is located within the micronemes of invasive malaria merozoites. *Cell* 63:141–153. [https://doi.org/10.1016/0092-8674\(90\)90295-p](https://doi.org/10.1016/0092-8674(90)90295-p).
- Treeck M, Struck NS, Haase S, Langer C, Herrmann S, Healer J, Cowman AF, Gilberger TW. 2006. A conserved region in the EBL proteins is implicated in microneme targeting of the malaria parasite *Plasmodium*

- falciparum*. J Biol Chem 281:31995–32003. <https://doi.org/10.1074/jbc.M606717200>.
7. Pattaradilokrat S, Culleton RL, Cheesman SJ, Carter R. 2009. Gene encoding erythrocyte binding ligand linked to blood stage multiplication rate phenotype in *Plasmodium yoelii yoelii*. Proc Natl Acad Sci U S A 106:7161–7166. <https://doi.org/10.1073/pnas.0811430106>.
  8. Otsuki H, Kaneko O, Thongkukiatkul A, Tachibana M, Iriko H, Takeo S, Tsuboi T, Torii M. 2009. Single amino acid substitution in *Plasmodium yoelii* erythrocyte ligand determines its localization and controls parasite virulence. Proc Natl Acad Sci U S A 106:7167–7172. <https://doi.org/10.1073/pnas.0811313106>.
  9. Pattaradilokrat S, Cheesman SJ, Carter R. 2008. Congenicity and genetic polymorphism in cloned lines derived from a single isolate of a rodent malaria parasite. Mol Biochem Parasitol 157:244–247. <https://doi.org/10.1016/j.molbiopara.2007.10.011>.
  10. Kegawa Y, Asada M, Ishizaki T, Yahata K, Kaneko O. 2018. Critical role of erythrocyte binding-like protein of the rodent malaria parasite *Plasmodium yoelii* to establish an irreversible connection with the erythrocyte during invasion. Parasitol Int 67:706–714. <https://doi.org/10.1016/j.parint.2018.07.006>.
  11. Iyer JK, Amaladoss A, Genesan S, Ganesan S, Preiser PR. 2007. Variable expression of the 235 kDa rhoptry protein of *Plasmodium yoelii* mediate host cell adaptation and immune evasion. Mol Microbiol 65:333–346. <https://doi.org/10.1111/j.1365-2958.2007.05786.x>.
  12. Freeman RR, Trejdosiewicz AJ, Cross GA. 1980. Protective monoclonal antibodies recognising stage-specific merozoite antigens of a rodent malaria parasite. Nature 284:366–368. <https://doi.org/10.1038/284366a0>.
  13. Lopatnicki S, Maier AG, Thompson J, Wilson DW, Tham WH, Triglia T, Gout A, Speed TP, Beeson JG, Healer J, Cowman AF. 2011. Reticulocyte and erythrocyte binding-like proteins function cooperatively in invasion of human erythrocytes by malaria parasites. Infect Immun 79:1107–1117. <https://doi.org/10.1128/IAI.01021-10>.
  14. Bapat D, Huang X, Gunalan K, Preiser PR. 2011. Changes in parasite virulence induced by the disruption of a single member of the 235 kDa rhoptry protein multigene family of *Plasmodium yoelii*. PLoS One 6:e20170. <https://doi.org/10.1371/journal.pone.0020170>.
  15. Fahey JR, Spitalny GL. 1984. Virulent and nonvirulent forms of *Plasmodium yoelii* are not restricted to growth within a single erythrocyte type. Infect Immun 44:151–156.
  16. Hisaeda H, Maekawa Y, Iwakawa D, Okada H, Himeno K, Kishihara K, Tsukumo S, Yasutomo K. 2004. Escape of malaria parasites from host immunity requires CD4+ CD25+ regulatory T cells. Nat Med 10:29–30. <https://doi.org/10.1038/nm975>.
  17. Li J, Pattaradilokrat S, Zhu F, Jiang H, Liu S, Hong L, Fu Y, Koo L, Xu W, Pan W, Carlton JM, Kaneko O, Carter R, Wootton JC, Su XZ. 2011. Linkage maps from multiple genetic crosses and loci linked to growth-related virulent phenotype in *Plasmodium yoelii*. Proc Natl Acad Sci U S A 108:E374–E382. <https://doi.org/10.1073/pnas.1102261108>.
  18. Wu J, Tian L, Yu X, Pattaradilokrat S, Li J, Wang M, Yu W, Qi Y, Zeituni AE, Nair SC, Crampton SP, Orandle MS, Bolland SM, Qi CF, Long CA, Myers TG, Coligan JE, Wang R, Su XZ. 2014. Strain-specific innate immune signaling pathways determine malaria parasitemia dynamics and host mortality. Proc Natl Acad Sci U S A 111:E511–E520. <https://doi.org/10.1073/pnas.1316467111>.
  19. Wu J, Cai B, Sun W, Huang R, Liu X, Lin M, Pattaradilokrat S, Martin S, Qi Y, Nair SC, Bolland S, Cohen JL, Austin CP, Long CA, Myers TG, Wang RF, Su XZ. 2015. Genome-wide analysis of host-*Plasmodium yoelii* interactions reveals regulators of the type I interferon response. Cell Rep 12:661–672. <https://doi.org/10.1016/j.celrep.2015.06.058>.
  20. Mutungi JK, Yahata K, Sakaguchi M, Kaneko O. 2015. Isolation of invasive *Plasmodium yoelii* merozoites with a long half-life to evaluate invasion dynamics and potential invasion inhibitors. Mol Biochem Parasitol 204:26–33. <https://doi.org/10.1016/j.molbiopara.2015.12.003>.
  21. Zhang C, Xiao B, Jiang Y, Zhao Y, Li Z, Gao H, Ling Y, Wei J, Li S, Lu M, Su XZ, Cui H, Yuan J. 2014. Efficient editing of malaria parasite genome using the CRISPR/Cas9 system. mBio 5:e01414-14. <https://doi.org/10.1128/mBio.01414-14>.
  22. Ferru E, Giger K, Pantaleo A, Campanella E, Grey J, Ritchie K, Vono R, Turrini F, Low PS. 2011. Regulation of membrane-cytoskeletal interactions by tyrosine phosphorylation of erythrocyte band 3. Blood 117:5998–6006. <https://doi.org/10.1182/blood-2010-11-317024>.
  23. Pantaleo A, Ferru E, Carta F, Mannu F, Giribaldi G, Vono R, Lepedda AJ, Pippia P, Turrini F. 2010. Analysis of changes in tyrosine and serine phosphorylation of red cell membrane proteins induced by *P. falciparum* growth. Proteomics 10:3469–3479. <https://doi.org/10.1002/pmic.201000269>.
  24. Schwartz RS, Olson JA, Raventos-Suarez C, Yee M, Heath RH, Lubin B, Nagel RL. 1987. Altered plasma membrane phospholipid organization in *Plasmodium falciparum*-infected human erythrocytes. Blood 69:401–407. <https://doi.org/10.1182/blood.V69.2.401.401>.
  25. Banerjee D, Saha S, Basu S, Chakrabarti A. 2008. Porous red cell ultrastructure and loss of membrane asymmetry in a novel case of hemolytic anemia. Eur J Haematol 81:399–402. <https://doi.org/10.1111/j.1600-0609.2008.01153.x>.
  26. Buffet PA, Safeukui I, Deplaine G, Brousse V, Prendki V, Thellier M, Turner GD, Mercereau-Pujalon O. 2011. The pathogenesis of *Plasmodium falciparum* malaria in humans: insights from splenic physiology. Blood 117:381–392. <https://doi.org/10.1182/blood-2010-04-202911>.
  27. Lang F, Qadri SM. 2012. Mechanisms and significance of eryptosis, the suicidal death of erythrocytes. Blood Purif 33:125–130. <https://doi.org/10.1159/000334163>.
  28. Lang E, Lang F. 2015. Mechanisms and pathophysiological significance of eryptosis, the suicidal erythrocyte death. Semin Cell Dev Biol 39:35–42. <https://doi.org/10.1016/j.semcdb.2015.01.009>.
  29. Eda S, Sherman IW. 2002. Cytoadherence of malaria-infected red blood cells involves exposure of phosphatidylserine. Cell Physiol Biochem 12:373–384. <https://doi.org/10.1159/000067908>.
  30. Greenberg ME, Sun M, Zhang R, Febbraio M, Silverstein R, Hazen SL. 2006. Oxidized phosphatidylserine-CD36 interactions play an essential role in macrophage-dependent phagocytosis of apoptotic cells. J Exp Med 203:2613–2625. <https://doi.org/10.1084/jem.20060370>.
  31. Fadok VA, Warner ML, Bratton DL, Henson PM. 1998. CD36 is required for phagocytosis of apoptotic cells by human macrophages that use either a phosphatidylserine receptor or the vitronectin receptor (alpha V beta 3). J Immunol 161:6250–6257.
  32. Hanson QM, Barb AW. 2015. A perspective on the structure and receptor binding properties of immunoglobulin G Fc. Biochemistry 54:2931–2942. <https://doi.org/10.1021/acs.biochem.5b00299>.
  33. Gaur D, Mayer DC, Miller LH. 2004. Parasite ligand-host receptor interactions during invasion of erythrocytes by *Plasmodium* merozoites. Int J Parasitol 34:1413–1429. <https://doi.org/10.1016/j.ijpara.2004.10.010>.
  34. Tham WH, Healer J, Cowman AF. 2012. Erythrocyte and reticulocyte binding-like proteins of *Plasmodium falciparum*. Trends Parasitol 28:23–30. <https://doi.org/10.1016/j.pt.2011.10.002>.
  35. Scully EJ, Kanjee U, Duraisingh MT. 2017. Molecular interactions governing host-specificity of blood stage malaria parasites. Curr Opin Microbiol 40:21–31. <https://doi.org/10.1016/j.mib.2017.10.006>.
  36. Le Bon A, Schiavoni G, D'Agostino G, Gresser I, Belardelli F, Tough DF. 2001. Type I interferons potentially enhance humoral immunity and can promote isotype switching by stimulating dendritic cells in vivo. Immunity 14:461–470. [https://doi.org/10.1016/S1074-7613\(01\)00126-1](https://doi.org/10.1016/S1074-7613(01)00126-1).
  37. Webb LM, Lundie RJ, Borger JG, Brown SL, Connor LM, Cartwright AN, Dougall AM, Wilbers RH, Cook PC, Jackson-Jones LH, Phythian-Adams AT, Johansson C, Davis DM, Dewals BG, Ronchese F, MacDonald AS. 2017. Type I interferon is required for T helper (Th) 2 induction by dendritic cells. EMBO J 36:2404–2418. <https://doi.org/10.15252/embj.201695345>.
  38. Urban BC, Ferguson DJ, Pain A, Willcox N, Plebanski M, Austyn JM, Roberts DJ. 1999. *Plasmodium falciparum*-infected erythrocytes modulate the maturation of dendritic cells. Nature 400:73–77. <https://doi.org/10.1038/21900>.
  39. Urban BC, Willcox N, Roberts DJ. 2001. A role for CD36 in the regulation of dendritic cell function. Proc Natl Acad Sci U S A 98:8750–8755. <https://doi.org/10.1073/pnas.151028698>.
  40. Bernabeu M, Smith JD. 2017. EPCR and malaria severity: the center of a perfect storm. Trends Parasitol 33:295–308. <https://doi.org/10.1016/j.pt.2016.11.004>.
  41. Winograd E, Sherman IW. 2004. Malaria infection induces a conformational change in erythrocyte band 3 protein. Mol Biochem Parasitol 138:83–87. <https://doi.org/10.1016/j.molbiopara.2004.07.008>.
  42. Giribaldi G, Ulliers D, Mannu F, Arese P, Turrini F. 2001. Growth of *Plasmodium falciparum* induces stage-dependent haemichrome formation, oxidative aggregation of band 3, membrane deposition of complement and antibodies, and phagocytosis of parasitized erythrocytes. Br J Haematol 113:492–499. <https://doi.org/10.1046/j.1365-2141.2001.02707.x>.
  43. Mankelov TJ, Satchwell TJ, Burton NM. 2012. Refined views of multi-

- protein complexes in the erythrocyte membrane. *Blood Cells Mol Dis* 49:1–10. <https://doi.org/10.1016/j.bcmd.2012.03.001>.
44. Kina T, Ikuta K, Takayama E, Wada K, Majumdar AS, Weissman IL, Katsura Y. 2000. The monoclonal antibody TER-119 recognizes a molecule associated with glycophorin A and specifically marks the late stages of murine erythroid lineage. *Br J Haematol* 109:280–287. <https://doi.org/10.1046/j.1365-2141.2000.02037.x>.
  45. Goel VK, Li X, Chen H, Liu SC, Chishti AH, Oh SS. 2003. Band 3 is a host receptor binding merozoite surface protein 1 during the *Plasmodium falciparum* invasion of erythrocytes. *Proc Natl Acad Sci U S A* 100:5164–5169. <https://doi.org/10.1073/pnas.0834959100>.
  46. Karunajeewa H, Lim C, Hung TY, Ilett KF, Denis MB, Socheat D, Davis TM. 2004. Safety evaluation of fixed combination piperazine plus dihydroartemisinin (Artekin(R)) in Cambodian children and adults with malaria. *Br J Clin Pharmacol* 57:93–99. <https://doi.org/10.1046/j.1365-2125.2003.01962.x>.
  47. Foley M, Tilley L, Sawyer WH, Anders RF. 1991. The ring-infected erythrocyte surface antigen of *Plasmodium falciparum* associates with spectrin in the erythrocyte membrane. *Mol Biochem Parasitol* 46:137–147. [https://doi.org/10.1016/0166-6851\(91\)90207-m](https://doi.org/10.1016/0166-6851(91)90207-m).
  48. Pei X, Guo X, Coppel R, Bhattacharjee S, Halder K, Gratzer W, Mohandas N, An X. 2007. The ring-infected erythrocyte surface antigen (RESA) of *Plasmodium falciparum* stabilizes spectrin tetramers and suppresses further invasion. *Blood* 110:1036–1042. <https://doi.org/10.1182/blood-2007-02-076919>.
  49. Martin-Jaurar L, Ferrer M, Calvo M, Rosanas-Urgell A, Kalko S, Graewe S, Soria G, Cortadellas N, Ordi J, Planas A, Burns J, Heussler V, del Portillo HA. 2011. Strain-specific spleen remodelling in *Plasmodium yoelii* infections in BALB/c mice facilitates adherence and spleen macrophage-clearance escape. *Cell Microbiol* 13:109–122. <https://doi.org/10.1111/j.1462-5822.2010.01523.x>.
  50. Yu X, Cai B, Wang M, Tan P, Ding X, Wu J, Li J, Li Q, Liu P, Xing C, Wang HY, Su XZ, Wang RF. 2016. Cross-regulation of two type I interferon signaling pathways in plasmacytoid dendritic cells controls anti-malaria immunity and host mortality. *Immunity* 45:1093–1107. <https://doi.org/10.1016/j.immuni.2016.10.001>.
  51. Ogun SA, Tewari R, Otto TD, Howell SA, Knuepfer E, Cunningham DA, Xu Z, Pain A, Holder AA. 2011. Targeted disruption of py235ebp-1: invasion of erythrocytes by *Plasmodium yoelii* using an alternative Py235 erythrocyte binding protein. *PLoS Pathog* 7:e1001288. <https://doi.org/10.1371/journal.ppat.1001288>.
  52. Lacerda-Queiroz N, Riteau N, Eastman RT, Bock KW, Orandle MS, Moore IN, Sher A, Long CA, Jankovic D, Su XZ. 2017. Mechanism of splenic cell death and host mortality in a *Plasmodium yoelii* malaria model. *Sci Rep* 7:10438. <https://doi.org/10.1038/s41598-017-10776-2>.
  53. Nair SC, Xu R, Pattaradilokrat S, Wu J, Qi Y, Zilversmit M, Ganesan S, Nagarajan V, Eastman RT, Orandle MS, Tan JC, Myers TG, Liu S, Long CA, Li J, Su XZ. 2017. A *Plasmodium yoelii* HECT-like E3 ubiquitin ligase regulates parasite growth and virulence. *Nat Commun* 8:223. <https://doi.org/10.1038/s41467-017-00267-3>.